Exp Brain Res (1997) 115:47–60

RESEARCH ARTICLE

Jacqueline P. Gottlieb · Asaf Keller

Intrinsic circuitry and physiological properties of pyramidal neurons in rat barrel cortex

Received: 24 May 1996 / Accepted: 7 November 1996

Abstract Pyramidal neurons in the rat posteromedial barrel subfield (PMBSF) were characterized physiologically and filled with biocytin in in vitro brain slices. Intrinsic axons belonging to supragranular neurons projected horizontally and vertically, arborizing in layers II/III and V, but had few or no projections to layers IV or VI. These axons projected horizontally for up to 2 mm, spanning two to seven barrel columns. Layer V neurons had more diffuse axon arbors that projected either vertically, arborizing in layers III to V, or horizontally, branching profusely in layers V and VI. The basal dendritic trees of neurons in layers II/III, V and VI spanned one or two barrel columns without being skewed toward particular barrel columns. Physiologically, regular-spiking neurons were classified as "RS_1" or "RS_2" according to their degree of late spike frequency adaptation. RS_1 neurons were found in superficial and deep layers, whereas RS_2 neurons were significantly more prevalent in the latter. Infragranular, but not supragranular neurons showed slow, inward rectification at hyperpolarized potentials. All neurons generated fast and medium afterhyperpolarizations following individual spikes; however, only infragranular pyramids had depolarizing afterpotentials interposed between the two afterhyperpolarizations. RS_1 neurons had larger cell bodies, longer total basal dendritic lengths, and more densely branched proximal dendritic trees than RS_2 neurons. These findings indicate that pyramidal neurons in the deep and superficial layers of the rat PMBSF have distinct patterns of intracortical axon arbors and distinct physiological properties. These features are probably involved in shaping and modulating the response properties of PMBSF neurons.

Key words Somatosensory cortex · Vibrissae · Biophysical properties · Biocytin · Posteromedial barrel subfield

J.P. Gottlieb · A. Keller (✉)[1]
Department of Anatomy and Cell Biology,
and Program in Neuroscience,
Uniformed Services University of the Health Sciences,
Bethesda, MD 20814, USA

Present address:
[1] Department of Anatomy and Neurobiology
University of Maryland School of Medicine,
685 W. Baltimore Street, Baltimore, MD 21201, USA;
Fax: +1–410–706–2512, e-mail: akeller@umabnet.ab.umd.edu

Introduction

The sensory system subserving the mystacial vibrissae (whiskers) of mammals is unique in that it samples information from an array of discrete peripheral receptor units. In certain rodent species, the whiskers map in a one-to-one, topographic manner onto corresponding arrays of discrete cellular aggregates at three consecutive relays: the trigeminal nucleus, the ventrobasal thalamic nucleus, and layer IV of the primary somatosensory cortex (reviewed in Jones and Diamond 1995). In the primary somatosensory cortex these aggregates are known as "barrels" and comprise the posteromedial barrel subfield (PMBSF; Woolsey and Van der Loos 1970).

A large number of studies have concentrated on the response properties of layer IV (barrel) neurons in the PMBSF. Neurons within a given barrel respond preferentially to deflections of one "principal" whisker (the "center" receptive field) and respond more weakly to several adjacent whiskers (the "surround" receptive field; for reviews see Armstrong-James 1995; Simons 1995). This spatial selectivity can be accounted for, in part, by the properties of afferents from the ventrobasal nucleus "barreloids" that terminate largely within a single corresponding barrel (Killackey and Leshin 1975; Senft and Woolsey 1991). In addition, local inhibition and the intrinsic biophysical properties of barrel neurons also influence their responses to whisker stimulation (Kyriazi et al. 1996).

Outside layer IV, however, much evidence points to the importance of local *excitatory* interactions in shaping neural responses. Even though thalamocortical afferents terminate almost exclusively in layers IV and Vb, neu-

rons outside these layers that are in vertical register with a barrel have the same center receptive field as that barrel's neurons, thus defining functional "barrel columns" that extend throughout the cortical layers (reviewed in Keller 1995). Neurons located outside the main thalamocortical termination zones in a given column (layers IV and Vb; Keller et al. 1985) respond at longer latencies to stimulation of their center receptive fields than do neurons located inside these zones, suggesting the existence of vertical intracortical relays (Armstrong-James and Fox 1987; Simons et al. 1992). Similarly, responses to stimulation of surround receptive fields have longer latencies and lower magnitudes than those to stimulation of center receptive fields, suggesting the operation of horizontal, inter-columnar pathways (Armstrong-James et al. 1992). Intracortical pathways are also crucial for the expression of plastic changes in the whisker map induced by selective, early whisker clipping (Fox 1994).

Despite the evidence regarding the importance of intracortical excitatory interactions, little is known about the local axon collaterals mediating these interactions – the axon collaterals belonging to pyramidal neurons within the PMBSF – nor about the intrinsic biophysical properties of these cells in relation to the functional organization of the PMBSF. Intrinsic pathways in the PMBSF were previously studied using small extracellular tracer injections or lesions (Bernardo et al. 1990; Chapin et al 1987; Hoeflinger et al 1995). While these studies revealed the general patterns of connectivity across the barrel field, they did not provide information about the axonal properties of individual neurons or about their biophysical properties.

In the present study we used an in vitro slice preparation to examine the somato-dendritic morphology, the intrinsic axon collaterals, and the biophysical properties of individual PMBSF pyramidal neurons in relation to the barrel and laminar architecture. Previous studies using extracellular dye injections showed that intrinsic connections in the PMBSF were oriented preferentially along barrel rows (Bernardo et al. 1990; Hoeflinger et al. 1995). We therefore chose a plane of slicing approximately parallel to barrel rows that seems to have preserved most of the intracortical arbors of the neurons we examined.

Materials and methods

In vitro experiments

All experimental procedures were performed in accordance with the *Principles of laboratory animal care* (NIH publication 86–23, revised 1985). Young adult Wistar rats of either sex (n=30, 24–37 days old) were anesthetized with chloral hydrate (3.5 mg/kg i.p.). Following whole-body immersion in ice water for 3–5 min, the brain was quickly removed and three or four slices, each 400 μm thick, were cut with a tissue chopper from the area containing the PMBSF of the left cortical hemisphere. Slices were cut in a frontal oblique plane, perpendicular to the dorsal aspect of the cortex and oriented posteromedially at 50° to the medial surface of the hemisphere. This plane was perpendicular to the one used by Welker and Woolsey (1974) to reveal individual barrel arcs in rat PMBSF and was thus expected to be approximately parallel to the barrel rows in this region. Slices were maintained in an interface-type chamber at 33±1°C and perfused at a rate of 1–2 ml/min with artificial cerebrospinal fluid (ACSF) composed of NaCl 124 mM, $NaHCO_3$ 26 mM, NaH_2PO_4 1.2 mM, KCl 3.2 mM, $MgSO_4$ 1.2 mM, CaCl 2.4 mM, and glucose 10 mM.

For intracellular recording and injection, micropipettes were pulled from borosilicate glass on a Flaming-Brown micropipette puller (Sutter Instruments, Novato, Calif.) and filled with solutions of 2% biocytin (Molecular Probes, Eugene, Ore.) in 1–2 M potassium acetate, to final resistances of 80–200 MΩ in the slice. Membrane voltage was measured and current was injected using an Axoprobe 1-A amplifier (Axon Instruments, Foster City, Calif.). Electrode signals were digitized at 20 kHz using the Superscope II software and a 12-bit MacAdios II analog-digital (A/D) board (GW Intruments, Somerville, Mass) and stored on hard disk.

Recordings were obtained from neurons in layers II/III and V/VI within the central mediolateral third of the slices, above the hippocampal fimbria and lateral ventricle. After achievement of stable membrane potentials of at least –58 mV, a series of 500-ms current pulses ranging from –0.5 to +1.5 nA were used to study the membrane properties of each cell. Bridge balance was continuously monitored throughout the recording and adjusted as necessary. Following recording, biocytin was injected from the micropipette using depolarizing pulses (0.8–1.2 nA, 500 ms, 0.5–1 Hz) superimposed on steady hyperpolarizing currents of 0.06–1.0 nA. Successful injections lasted 20–60 min and slices were maintained in the recording chamber for at least 1 h following each injection to allow transport of the dye to the most distal processes.

Histological processing

Slices containing stained neurons were fixed for 12–48 h in 4% paraformaldehyde (pH 7.4) at 4°C. They were then transferred to a phosphate buffer (PB; 0.1 M PO_4, 0.5 M NaCl) containing 30% sucrose until they sank, rapidly freeze-thawed twice on dry ice, and sectioned at 50 μm on a vibratome. Following a brief rinse to remove unbound aldehydes, sections were incubated for 20 min in 0.5% H_2O_2, rinsed for 15 min, and incubated sequentially in the A and B components of the Elite Standard ABC kit (Vector, Burlingame, Calif.; 30 min A, 30 min B, 30 min A, 30 min B). From the first rinses and up to this point the reactions were carried out in PB containing 2% Triton-X to further permeabilize the tissue and facilitate penetration of reagents. After two 15-min rinses in PBS the sections were incubated for 5–10 min in a solution containing 3–3′ diaminobenzidine (DAB; 0.7 mg/ml), urea H_2O_2 (1.6 mg/ml), and 0.01% nickel ammonium sulfate in 0.06 M TRIS buffer. Sections were then rinsed again, mounted on gelatin-coated slides, and air-dried. In initial experiments we found that barrels were often visible after the HRP-DAB reaction alone (see also Cauller and Connors 1994). To further intensify the DAB stain and the barrel outlines, sections were reacted for 3–5 min with 1% OsO_4 on the slides, rinsed, dehydrated, and coverslipped.

In vivo experiments

To ascertain that our plane of section was parallel to barrel rows, two additional animals were deeply anesthetized with chloral hydrate (3.5 mg/kg i.p.) and perfused transcardially with PB followed by 4% paraformaldehyde. The brains were then removed and the posterior portions of each hemisphere were blocked and sectioned at 50 μm in a plane similar to that used for slice preparation. Sections were then reacted for cytochrome oxidase histochemistry (Wong-Riley 1979) and two-dimensional reconstructions were obtained for the entire PMBSF. Barrels traced in adjacent sections were well aligned relative to each other, and comparison of individual sections with the full reconstruction showed that, in most cases, barrels recovered in any given section belonged to one row. Misalignments occurred most frequently in the anterolateral portion of the PMBSF where the curvature of barrel rows is most pronounced and individual sections cut across rows.

Such misalignments were never observed in the sections used for reconstructions of neurons recorded in vitro, indicating that the slices for these experiments were cut approximately parallel to the barrel rows. Because our thin sections were of comparable thickness to rat barrel septa (about 50 μm), we could not delineate precisely the boundaries between adjacent barrel rows. Reconstructions of individual neurons, therefore, could extend across, at most, two adjacent barrel rows.

Data analysis

Voltage records were analyzed off-line using the Superscope II software. Membrane resistances and time-constants were estimated from the voltage responses to small (0.05–0.1 nA) hyperpolarizing current pulses. Values of spike amplitudes and rise and fall times were obtained from the first spikes in trains elicited with currents equal to or slightly higher than rheobase currents. The onset and offset of spikes were marked with a user-controlled cursor at the points when membrane potential began to rise sharply, or returned to resting values, respectively.

Reconstructions were made using the Neurolucida reconstruction software (MicroBrightField, Colchester, Vt.). Barrel outlines were drawn at ×4 in each section in which they were clearly visible and mean contours were then drawn for each slice from the superimposed outlines. These mean contours were superimposed upon the two-dimensional neuronal reconstructions. A "barrel column" was defined as the tissue in vertical register with each mean contour, i.e., that bound by two lines tangent to the lateral edges of this contour. The upper and lower boundaries of the barrels were taken to represent the layer IV boundaries.

Biocytin-filled neurons were drawn at ×40. Two-dimensional reconstructions of dendritic and axon arbors were obtained from 4 to 7 adjacent sections (mean five sections, or about 250 μm). Most cell bodies were located about 100 μm deep to the top surface of the slice (i.e., in the second or third sections reconstructed; range 50–200 μm).

The most superficial and the deepest sections recovered from each slice (representing its cut surfaces) were examined for the presence of neuronal processes to estimate the degree to which these had been truncated during slice preparation. Neurons whose basal dendrites extended into these sections were considered excessively truncated and were excluded from analysis. Neurons whose apical (but not basal) dendrites extended to the cut surfaces of the slices were included in the analysis; however, conclusions about their apical dendrites were qualified. Sparse axonal projections were detected at the limit of the slice for most neurons. Such truncation of widespread axonal arbors is inevitable in a slice preparation. The limitations it imposes on our conclusions were discussed extensively in the Results and Discussion.

Numeric analyses and Sholl analyses (Sholl 1953) were carried out for each reconstructed neuron using the WinMorph software package (MicroBrightField, Colchester, Vt.). The Fisher exact probability test was used to test for differences in distributions with totals of less than 20 observations.

Results

All the neurons described in this report were spiny pyramidal cells with somata in layers II/III or V/VI of the PMBSF. We describe first the intracortical axon projections and dendritic arbors of these neurons in relation to the barrel architecture. We then report on these neurons' physiological properties and on some of their morphometric characteristics in relation to their physiological properties and laminar locations.

Figure 1A–C depicts photomicrographs of three biocytin-stained neurons representative of those selected for morphological analysis. As seen in the figure, the cell bodies and proximal processes of these neurons stained darkly and homogeneously, revealing networks of fine local axon collaterals as well as longer processes that could extend for several hundred microns in a single section (Fig. 1B). All labeled axons had a periodic beaded appearance, similar to that described in some other studies where they were interpreted as representing boutons en passant. However, because of the uncertainty in relating these structures to synaptic contacts (White 1989), we will not report on their distribution.

Neurons were included in the analysis only if they were located in the region of the large barrels (300–400 μm in diameter) that define the PMBSF (Welker and Woolsey 1974). Figure 1D shows, at lower magnification, an example of PMBSF barrels revealed by the HRP-DAB stain and OsO_4 intensification in a section containing a biocytin-stained neuron. In the following description we pay particular attention to the relationships between neuronal processes and barrel architecture, i.e., the barrels in layer IV and the tissue in vertical register with them – or "barrel columns" (see Materials and methods).

Seventeen neurons that had staining comparable with that shown in Fig. 1 were selected for reconstructions of both axonal and dendritic arbors. Eight of these were located in layers II/III (the supragranular, SG, layers), eight in layer V, and one in layer VI (the infragranular, IG, layers). In nine additional IG neurons (one in layer V and eight in layer VI), only the dendritic trees were considered sufficiently well filled with biocytin and were reconstructed.

Axonal and dendritic arbors

Supragranular neurons (n=8)

Reconstructions of representative SG neurons and their relation to PMBSF barrels are shown in Fig. 2. SG neurons usually were recorded in the lower half of the SG layers corresponding to layer III. Their apical dendrites originated from pyramidal-shaped cell bodies and branched along their entire lengths, from very close to the cell bodies and up to layer I. The basal dendritic trees formed skirts with maximum radii of 140–280 μm that were not skewed toward particular barrel columns. Thus, the basal dendrites of neurons located above barrel walls spanned two adjacent barrel columns (Fig. 2A), whereas those of neurons located closer to the center of a barrel column tended to remain within that column (Fig. 2B). The basal dendrites terminated in the SG layers and did not reach layer IV. It should be noted, however, that our sample did not include neurons located in the lowest portion of layer III, and we cannot exclude the possibility that basal dendrites of these neurons did project into layer IV.

The axons of SG neurons arborized extensively in layers II/III and/or V but avoided layer IV almost entire-

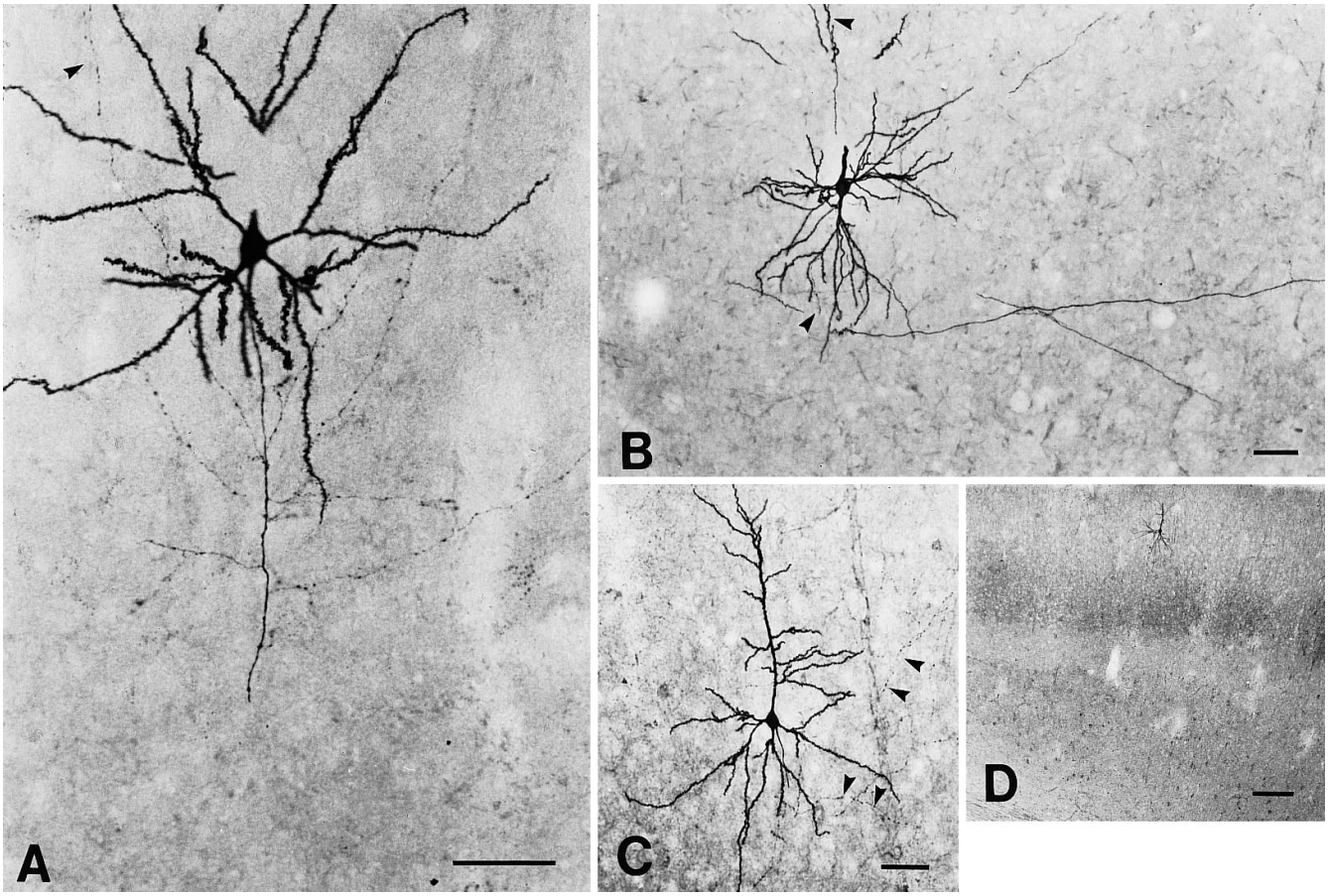

Fig. 1 **A–C** Photomicrographs of two supragranular (SG) neurons (**A,C**) and one layer V neuron (**B**) filled intracellularly with biocytin. The stain revealed local (**A–C**) and long horizontal (**B**) axon collaterals (*arrowheads*) in each neuron, as well as fine structural details including boutons and dendritic spines. *Scale bars* 50 μm. **D** Low-power photomicrograph showing a biocytin-filled neuron in the SG layers overlying several large barrels revealed by the HRP-DAB stain and OsO_4 intensification. *Scale bar* 200 μm

ly. The few axon branches observed in this layer were restricted to its upper or lower boundaries or passed through it to arborize in SG or IG layers (Fig. 2). Five SG neurons had extensive arbors in both layers II/III and V. In two neurons only SG, but no layer V arbors, were seen, despite good tissue preservation and good staining overall (e.g., Fig. 2D), suggesting that some SG neurons lack IG projections. In the remaining neuron the IG layers had been damaged during processing, making it impossible to judge the presence of a layer V projection.

Horizontal collaterals in layers II/III and V extended for 600–2000 μm, spanning two to seven barrel columns. Despite this large horizontal extent, however, the densest axon arborizations were restricted to the cells' parent barrel column and, sometimes, to one adjacent column, with more distant columns receiving many fewer and less branched collaterals. In the superficial layers, numerous vertical and oblique branches coursed within and immediately around the dendritic field of the neurons (Fig. 2), in close proximity to the neurons' dendritic branches (see also Fig. 1A,C). Occasionally, a single recurrent collateral arose from the layer V arbor, passed unbranched through layer IV, and formed a small terminal arbor in layers II/III adjacent to the edge of the SG arborization (Fig. 2A,B). Long axon collaterals sometimes projected from the main axon in layer V and traveled obliquely toward and through layer VI, where they occasionally gave off an additional horizontal branch (Fig. 2A,B).

Layer V neurons (n=8)

Seven of the reconstructed layer V neurons were located in the lower portion of this layer (sublamina Vb) and the remaining cell was located in its upper half (sublamina Va). The apical dendrites of layer V neurons ascended, branching sparsely, through layer V and terminated in layer IV (five neurons), in layers II/III (two neurons), or in layer I (one neuron). Two of the apical dendrites terminating in layer IV did so well within the series of reconstructed sections and were well stained at their tips, suggesting that they had not been truncated during slice or section preparation, nor had they been missed because of poor transport of dye to distal processes. However, we could not rule out the possibility that the apical dendrites of the remaining three neurons appeared to terminate be-

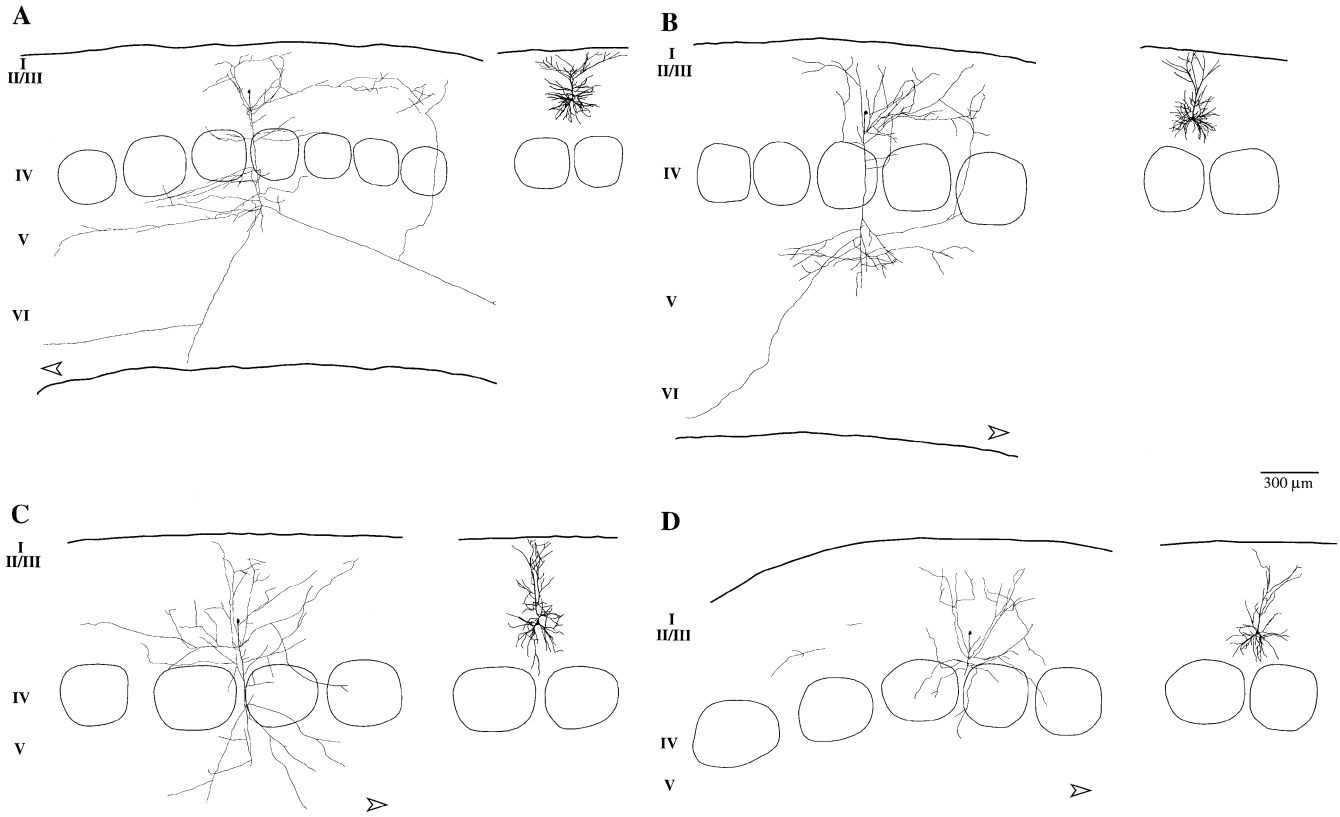

Fig. 2A–D Reconstructions of four SG neurons. *Left* portion of each panel, the axonal arbor; *right* the dendritic tree of each neuron, in relation to layer IV barrels. The barrel contours are means of superimposed barrel outlines drawn in several consecutive sections. Cortical layers are indicated by *Roman numerals*, and laminar boundaries occur approximately halfway between these numerals. The locations of the pial surface and the border of the white matter are indicated as *solid lines*. *Arrowheads* point in the posteromedial direction in each panel. Physiologically, all four neurons were classified as RS_1

low layers II/III because of such artifacts. Like SG neurons, layer V cells had basal dendritic arbors with maximal radii of 140–260 µm, which spanned one or at most two adjacent barrel columns and were not skewed toward particular columns (Fig. 3).

The axon collaterals of layer V neurons innervated predominantly layers V and VI, had sparser projections to layer IV, and sent only few collaterals to layers II/III. Extensive axon arbors of layer V neurons in the SG layers (such as those formed by SG neurons in layer V) were never observed.

The patterns of intracortical axon projections of layer V neurons were more varied than those of SG neurons. Some neurons formed predominantly vertical or oblique collaterals with a horizontal span of two to four barrel columns (Fig. 3A–C). They sometimes had a few horizontal collaterals that traveled, sparsely branched, for up to 1 mm (spanning four barrel columns) in lower layer V and layer VI (Fig. 3B). Other layer V neurons, in contrast, formed predominantly horizontal axonal plexi that spanned up to six barrel columns in layers V and VI (up to 2 mm; Fig. 3D). These neurons gave off only one or two vertical collaterals that branched in narrow domains in layers III and IV.

Layer VI neurons (n=8)

Four layer VI neurons had apical dendrites oriented toward the pial surface. These were sparsely branched in their proximal portions and ascended unbranched through layer V before terminating with two or three short ramifications in upper layer V. The remaining layer VI neurons had apical dendrites oriented obliquely or near horizontally (Fig. 4) or, in one case, toward the white matter. These apical dendrites branched throughout their length and always terminated within layer VI. The basal dendritic trees of layer VI neurons had similar dimensions to those of SG and layer V neurons and spanned one or two adjacent barrel columns.

Although several layer VI neurons had well-labeled dendritic processes, only one had an axonal arbor complete enough to warrant reconstruction (Fig. 4). We show the reconstructed axonal arbor of this neuron as a solitary example, but clearly can draw no general conclusions about the axonal arbors of layer VI neurons as a whole. The difficulty in obtaining well-labeled cells in this layer was probably due to the small, polymorphic somata characteristic of its cells and to the relatively low cell density in its lower portions (van Brederode and Snyder 1992; see also Agmon and Connors 1992). The axonal arbor of this cell extended across two barrel col-

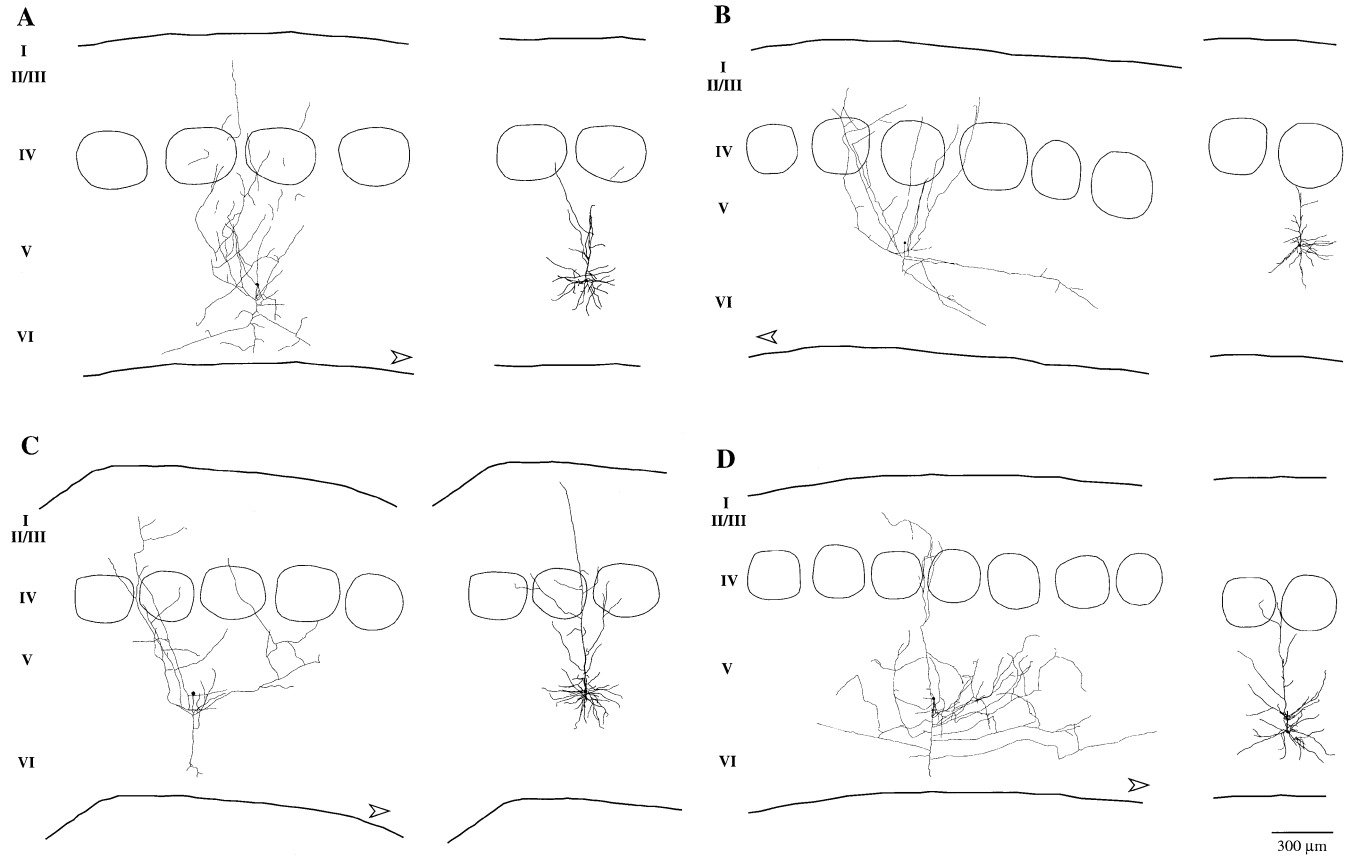

Fig. 3A–D Reconstructions of four layer V neurons. All conventions as in Fig. 2. The neuron in **C** was classified as RS_1, all others as RS_2

umns and slightly beyond the anterolateral border of the PMBSF and was almost entirely confined to layer VI. Only two branches left layer VI and, traveling close to each other, extended vertically and terminated in lower layer III.

Physiological properties

Physiological properties were analyzed in 21 neurons that had stable resting membrane potentials of at least –58 mV (–74.5±8.5 mV; mean±SD) and overshooting spikes of at least 66 mV (73.2±6.1 mV; mean±SD). Nine of these neurons were located in the SG layers, and 12 in the IG layers (11 in layer V and 1 in layer VI). We describe first the physiological properties noted in the entire sample and then the differences in physiological characteristics of SG versus IG neurons.

Firing patterns and afterpotentials

When injected with suprathreshold current pulses, all neurons responded in one of two distinct patterns, which are shown in Fig. 5. We refer to these groups as RS_1 and RS_2, a nomenclature first proposed by Connors and his

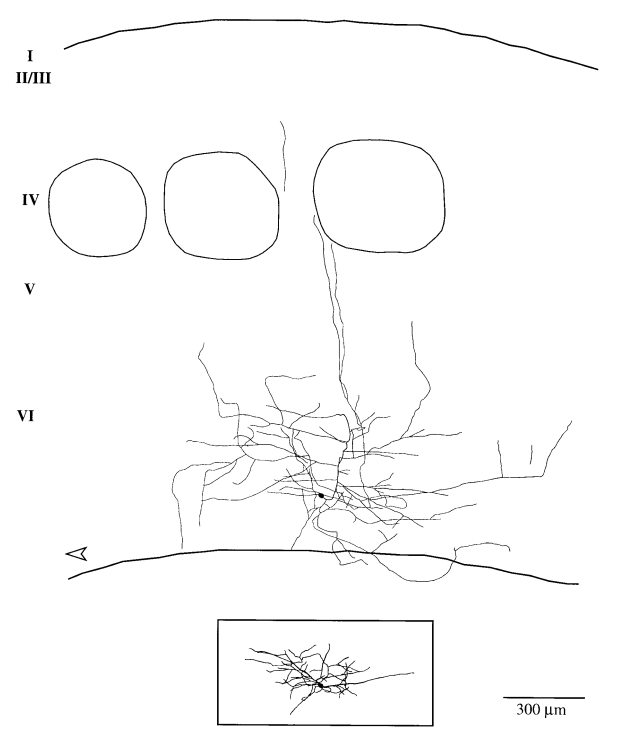

Fig. 4 Reconstruction of a layer VI neuron. The *top* shows the axonal arbor, barrels, and laminar architecture and the *inset at the bottom* shows the neuron's dendritic tree. All other conventions are as in Figs. 2 and 3

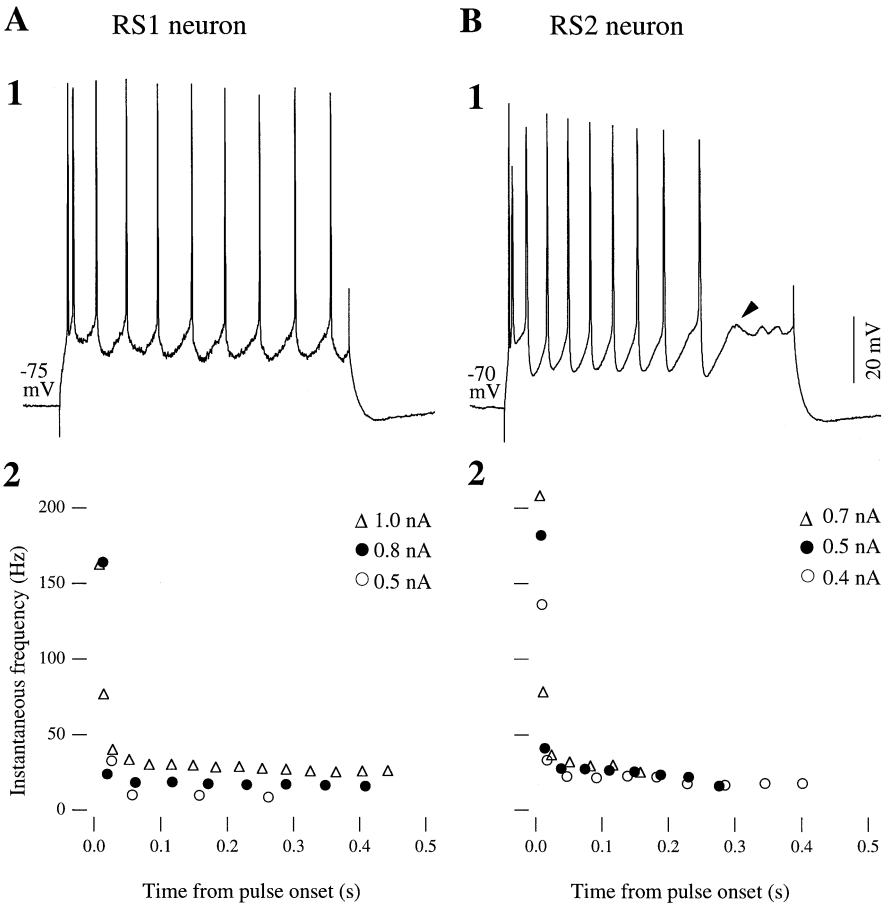

Fig. 5A, B Physiological properties of RS_1 and RS_2 neurons. The data in **A** are from a SG neuron with an adaptation ratio of 1.14 and that in **B** from a layer V neuron with a ratio of 1.67 (the lowest among RS_2 neurons; see text). Current pulses were 0.8 nA and 0.5 nA in **A**,*1* and **B**,*1*, respectively, and lasted 500 ms. The voltage *calibration bar* applies to both **A**,*1* and **B**,*1*. The lower portion of the figure (*2*) shows plots of the instantaneous firing rates elicited by different current pulses in the same neurons. *Filled circles* represent data obtained from the records shown in *1*. Note that the last spike (data point) occurs progressively earlier in the train as current intensity is increased in the RS_2 neuron, and the converse occurs in the RS_1 neuron. Rheobase was 0.5 nA for the neuron in **A** and 0.3 nA for the neuron in **B**. The morphological reconstruction of the neuron in **A** is shown in Fig. 2B, and more of its physiological properties are shown in Fig. 6

colleagues to describe regular-spiking neurons in the somatosensory cortex of the rat and mouse (Agmon and Connors 1992; Chagnac-Amitai and Connors 1989). Neurons in both groups generated high-frequency clusters of two to three spikes at the onset of their responses that adapted rapidly (within 50 ms) and were followed by a lower-frequency portion of the response. Following these initial adapting spikes, RS_1 cells generated trains of single spikes that lasted, with virtually no frequency adaptation, throughout long (500 ms) current pulses (Fig. 5A,1). Higher current intensities elicited a larger number of spikes with higher frequencies (Fig. 5A,2). In contrast, in RS_2 neurons the initial high-frequency spike cluster was followed by slowly adapting and often irregular spike trains (Fig. 5B,1). Higher current intensities did not produce higher-frequency firing and sometimes led to gradual suppression of spiking (Fig. 5B,2). Small depolarizing waves were often seen during this suppression (Fig. 5B,1, arrowheads) and could trigger spikes at irregular intervals. Injections of constant hyperpolarizing or depolarizing current (–0.1 to +0.1 nA) superimposed on the suprathreshold current pulses changed the firing frequencies, but not the firing patterns of neurons.

In order to quantify the degree of adaptation across different neurons and to ensure correct classification in each case, we calculated an “adaptation ratio” for each cell, defined as the ratio of the 9th to the 3rd interspike intervals in a representative record containing 10–12 spikes. These records were usually obtained at about 150% of rheobase current; increasing the current intensity did not alter the classification of cells. Neurons with ratios close to 1 (indicating little or no late adaptation; range 0.98–1.23, n=13) were counted as RS_1, whereas those with greater ratios (1.67–8.67, n=5) were counted as RS_2. We classified as RS_2 three additional neurons that, because of their pronounced adaptation, never generated ten spikes in a single train. The RS_1 neuron whose responses are shown in Fig. 5A had a ratio of 1.14; the neuron shown in Fig. 5B was the“least adapting” of the RS_2 group, with a ratio of 1.67. Using this measure, 13 neurons were classified as RS_1 and eight as RS_2.

We recorded one additional neuron that clearly differed from the two classes described above in that it generated spike bursts typical of intrinsically bursting neurons previously described in the somatosensory cortex (Chagnac-Amitai and Connors 1989; Connors et al. 1982; McCormick et al. 1985). Unlike the initial spike clusters generated by RS_1 and RS_2 neurons, these bursts were elicited at just-suprathreshold current intensities and occurred repeatedly throughout the current pulse. This neuron was located in lower layer V and its apical dendrite terminated in layer I, consistent with the morphology of intrinsically bursting neurons described by Chagnac-Amitai et al.(1990). This cell will not be described further in this report.

Table 1 Physiological properties of posteromedial barrel subfield neurons afterpotentials (*DAPs* depolarizing, *SG* supragranular, *IG* infragranular)

	SG neurons	IG neurons	RS_1 neurons	RS_2 neurons
Resting potential (mV)				
Mean	−74.5±8.5	−75.7±3.4	−75.5±7.5	−74.7±2.4
Range	−58 to −89	−71 to −81	−58 to −89	−72 to −78
n	9	12	13	8
Input resistance (MW)				
Mean	47.0±11.8	52.4±21.6	48.6±18.0	52.5±17.9
Range	29–67	21–81	31–76	21–69
n	9	11	13	7
Time constant (ms)				
Mean	13.3±6.1	12.6±4.25	14.21±3.4	10.6±3.5
Range	8–20	8–20	9–20	8–16
n	9	11	13	7
Spike threshold (mV)				
Mean	−52.2±4.7	−55.9±5.6	−55.0±6.2	−53.2±4.1
Range	−47 to −58	−44 to −58	−50 to −66	−47 to −58
n	9	11	13	7
Rheobase (nA)				
Mean	0.4±0.1	0.3±0.2	0.3±0.1	0.4±0.2
Range	0.1–0.5	0.1–0.5	0.1–0.4	0.1–0.6
n	8	11	12	8
Spike amplitude1 (mV)				
Mean	73.2±6.1 (9)	68.9±7.2	72.6±7.4	67.7±5.2
Range	66–78	56–81	60–84	56–72
n	9	12	13	8
Spike width (ms)				
Mean	2.0±0.3	1.93±0.6	1.9±0.3	2.0±0.7
Range	1.4–2.2	1.1–3.1	1.4–2.2	1.1–3.1
n	9	12	13	8
Fall/rise time[a]				
Maen	3.1±0.9	2.03±0.6	2.6±0.5	2.3±1.3
Range	2.2–5.2	1.0–2.8	2.0–3.5	1.0–5.2
n	9	12	13	8
Depol. sag (%)[b]				
n	1/8**	8/10	5/11	4/7
%	13	80**	45	57
Hyperpol. sag (%)[c]				
n	8/8	6/8	9/115/5	
%	100	75	82	100
DAPs (%)[d]				
n	1/8	8/12	6/12	3/8
%	13	67	50	38

** $P<0.05$ relative to SG or IG neurons, the Fisher exact probability test. In all but the last three rows data represent mean±SD. In the last three rows data represent number of cells expressing properties/number of observations (percentage)

[a] Spike amplitude was measured from Vm to peak, and spike duration was measured from spike beginning to end (see Materials and methods). Fall/rise time is the ratio time from spike peak to spike end:time from spike threshold to spike peak

[b] Number of neurons showing sag of at least 1 mV above the potential reached close to the onset of a –0.3 nA current pulse

[c] Number of neurons showing sag of at least 1 mV below the potential reached close to the onset of a depolarizing current pulse of 0.1 nA below rheobase

[d] Number of neurons showing DAPs (see text)

Spike afterpotentials

Spikes elicited by suprathreshold current pulses were followed by three distinct afterpotentials: a fast hyperpolarization that continued without inflection from the spike repolarization phase (f-AHP), a depolarizing afterpotential (DAP) following the f-AHP, and a later, medium-duration afterhyperpolarization (m-AHP; Fig. 6A,3, B,3). The m-AHP amplitude tended to increase with successive spikes. In contrast, DAPs were most prominent after the first spikes in a train, or after spikes elicited with low, just-suprathreshold currents.

Subthreshold responses

In response to hyperpolarizing current pulses, the membrane potential of some neurons "sagged" from an initial value to more depolarized steady-state levels (Fig. 6B,1,2). Such depolarizing sags occurred within the first 100 ms of the responses, were visible at relatively small hyperpolarizations (less than –5 mV from rest), and increased with increased amplitudes of injected current. Depolarizing overshoots were seen after current offset, increased with current (and sag) amplitude, and could trigger one or two spikes if sufficiently large.

In response to subthreshold depolarizing current pulses, almost all neurons generated hyperpolarizing sags, i.e., their initial membrane potentials fell to lower steady-state levels within 100 ms (Fig. 6A,B, Table 1). The initial responses, and, to a much lesser extent, the la-

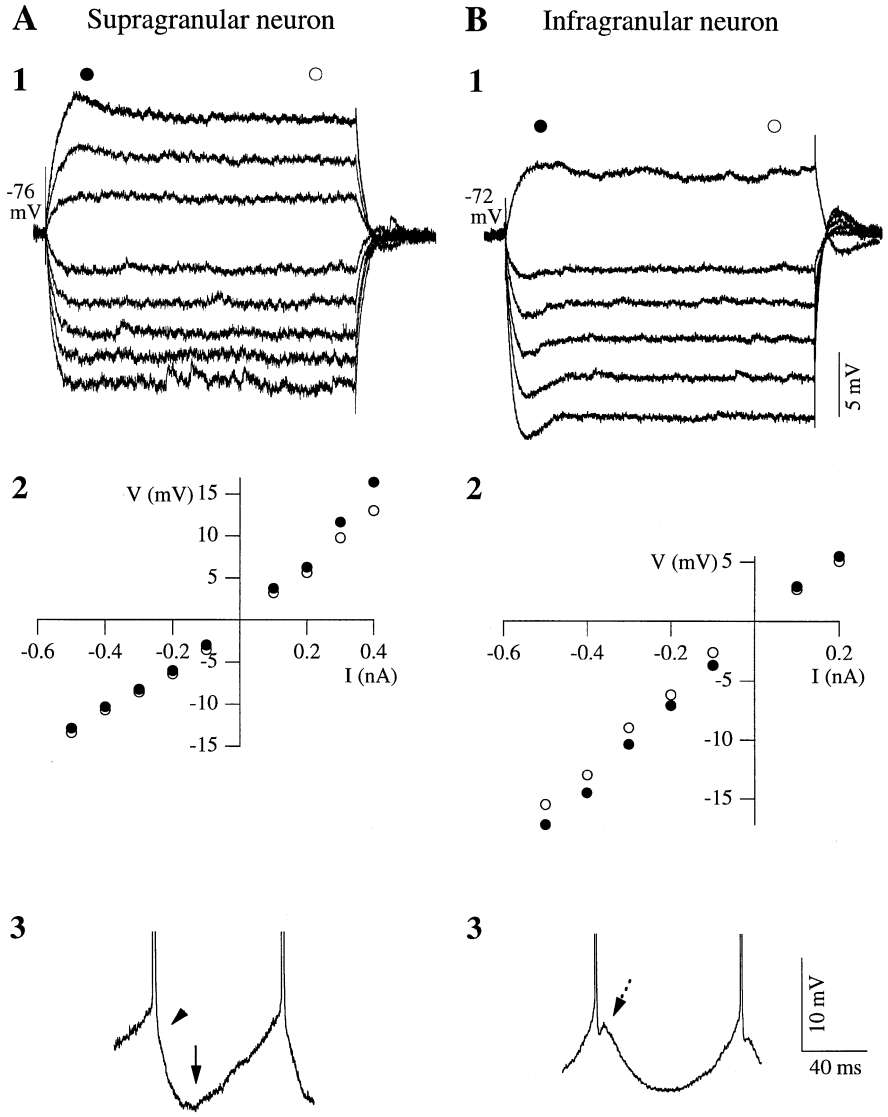

Fig. 6A, B Subthreshold responses and spike afterpotentials of representative SG and IG neurons. Data in **A** and **B** are from two RS_1 neurons with adaptation ratios of 1.14 and 1.27, respectively, and their morphologies are depicted in Figs. 2B and 4, respectively. *1* Subthreshold responses elicited with hyperpolarizing current steps (500 ms duration) between –0.5 and –0.1 nA, in 0.1-nA increments, in both **A** and **B**, and with depolarizing current steps of 0.1, 0.2, and 0.3 nA in **A** and of 0.2 nA in **B**. Rheobase was 0.5 nA for the neuron in **A** and 0.3 nA for that in **B**. *2 I–V* plots constructed for each neuron from the peak of the initial hyperpolarizing or depolarizing voltages (*filled circles*) and from the response near the end of each current pulse (*open circles*). *3* Each spike elicited from the SG neuron was followed by fast- and medium-duration afterhyperpolarizations (*arrowhead* and *solid arrow*, respectively). The IG neuron also generated DAPs (*broken arrow*) between the f- and m-afterhyperpolarization. Spikes were elicited with 0.8 nA in **A**,3 and 0.4 nA in **B**,3. *Scale bar* applies to **A** and **B**. Spike amplitudes are truncated

ter phases of the responses, were associated with inward rectification (Fig. 6A,1, B,1).

Differences in physiological properties of SG and IG neurons

As can be seen in Table 1, SG and IG neurons did not differ significantly in a number of membrane properties (resting potential, input resistance, and time constant) or spike parameters (spike rheobase, threshold, amplitude, rise and fall times, and width). However, three major physiological properties distinguished SG from IG neurons.

First, whereas SG neurons were almost exclusively of the RS_1 type, IG neurons were about equally divided among the RS_1 and RS_2 groups. Using the adaptation ratio defined above, eight SG neurons were RS_1 and one was an RS_2, whereas in the IG layers, five neurons were classified as RS_1 and seven as RS_2. These distributions were significantly different from each other ($P<0.05$). Second, the prevalence of depolarizing sags was significantly greater in IG than in SG neurons. Sags were seen in eight of ten IG neurons but in only one of eight SG neurons tested ($P<0.05$; Fig. 6, Table 1). As shown in Fig. 6A,1,2, SG neurons maintained stable voltage levels throughout long hyperpolarizing current pulses and showed no potential overshoots at pulse offset. Finally, DAPs were seen in most IG neurons (8/12) but in only one of eight SG neurons ($P<0.05$; Fig. 6A,3, B3; Table 1).

It should be noted that the presence of a depolarizing sag and DAPs were not associated with a particular repetitive firing pattern (Table 1). RS_1 as well as RS_2 neurons showed the distinct subthreshold responses and spike afterpotentials characteristic of neurons in their parent layer. For instance, the responses in A and B of Fig. 6 were taken from two RS_1 neurons with very similar adaptation ratios (1.14 and 1.27, respectively).

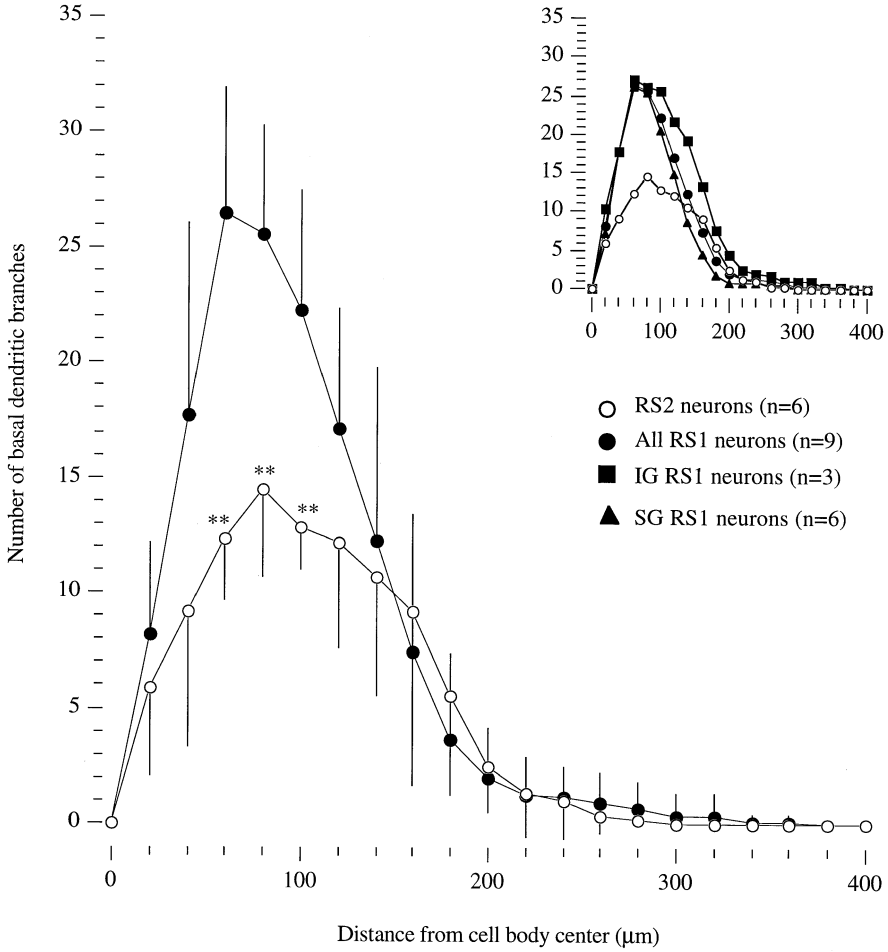

Fig. 7 Sholl analysis of the basal dendrites of RS_1 and RS_2 neurons. The larger graph shows the number of basal dendritic branches (mean and SDs) at increasing distances (20-μm increments) from the parent cell bodies. Values obtained at 60, 80, and 100 μm (*stars*) were significantly different for RS_1 and RS_2 neurons ($P<0.05$, Student's two-tailed *t*-test). The *inset* compares the results of the Sholl analysis of basal dendrites for RS_1 neurons located in SG and IG layers, with the data shown in the larger plot (mean values only). There were no significant differences between RS_1 neurons in the SG and IG layers

Table 2 Morphometric measurements of posteromedial barrel subfield neurons

		RS1 neurons	RS2 neurons	SG RS1 neurons	IG RS1 neurons
Cell body area (mm2)					
	Mean	243.9±39.1**	190.5±41.7	233.6±45.1**	264.5±7.9**
	Range	158 to 267	134 to 236	178 to 275	158 to 267
	n	9	7	6	3
Number of primary basal dendrites					
	Mean	6.9±2.4	6.1±1.8	6.8±2.9	7.0±1.0
	Range	4 to 11	4 to 8	4 to 11	6 to 8
	n	9	7	6	3
Total length of basal dendrites (mm)					
	Mean	4.2±1.1**	2.9±0.6	3.6±0.7	5.3±1.0**
	Range	2.5 to 6.3	1.9 to 3.6	2.5 to 4.9	4.3 to 6.3
	n	9	6	6	3
Number of basal dendrites at:[a]					
60 mm	Mean	26.4±5.5	12.3±2.7	26.2±5.6**	27.0±6.3**
	Range	20 to 34	10 to 17	20 to 30	22 to 34
	n	9	6	6	3
80 mm	Mean	25.6±4.7	14.5±3.9	25.3±5.5	26.0±3.5**
	Range	19 to 35	10 to 20	19 to 35	24 to 30
	n	9	6	6	3
100 mm	Mean	22.2±5.2	12.8±1.9	20.5±3.9**	25.7±6.7**
	Range	14 to 33	10 to 15	14 to 26	20 to 33
	n	9	6	6	3

Mean±SD; *n* is number of cells
** $P<0.05$ relative to RS_2 neurons, Student's 2-tailed *t*-test
[a] From Sholl analysis of dendritic intersections

Morphometric analyses

Reconstructions of dendritic trees and morphometric measurements were obtained for 17 physiologically identified neurons, including 9 RS_1 cells (6 in the SG layers, 2 in layer V, and one in layer VI), 7 RS_2 cells (1 in the SG layers and 6 in layer V), and 1 intrinsic bursting neuron.

As shown in Table 2, RS_1 neurons had significantly larger cell bodies and total basal dendritic length than RS_2 neurons. Sholl analysis of the basal dendrites of RS_1 and RS_2 neurons (Fig. 7, Table 2) showed that RS_1 neurons had significantly more dendritic branches than RS_2 neurons at distances of 60, 80, and 100 μm from the parent somata. This difference in branching patterns probably accounted for the difference in total dendritic length, as RS_1 and RS_2 neurons had similar numbers of primary basal dendrites and similar overall spans of the basal dendritic trees (Fig. 7, Table 2). The difference in basal dendritic branching patterns can also be appreciated by comparing the dendritic arbors of the neurons in Figs. 2 and 3C (all RS_1 neurons) with those shown in Fig. 3A,B,D (RS_2 neurons). RS_1 neurons located in SG and IG layers did not differ from each other in any of the morphometric parameters examined (Table 2, Fig. 7, inset). Thus, the morphometric differences we describe were associated with physiological type, and not with laminar location.

As described above, the apical dendrites of layer V neurons usually terminated in layers II–IV, and only one neuron – the intrinsically bursting cell – had an apical dendrite that arborized in layer I. In order to minimize possible artifacts due to truncation of the dendritic tree, Sholl analysis of apical dendrites was restricted to the proximal 500 μm – a range that included the entire apical dendritic arbors of SG neurons and of some IG neurons. This analysis revealed no significant differences between RS_1 and RS_2 cells, nor between SG and IG neurons.

Discussion

As the main source of intrinsic excitatory drive in the neocortex, pyramidal neurons are primary determinants of neocortical function (Gutnick and Crill 1995). Physiologically, the majority of pyramidal neurons in layers II–VI are classified as RS cells – those that generate trains of single action potentials in response to intracellular current injections (Gutnick and Crill 1995; McCormick et al. 1985). Our data demonstrate that RS neurons in the PMBSF cannot be regarded as a homogeneous class, as their morphologies and intrinsic biophysical properties vary both according to laminar location and within a given layer. SG RS neurons are of the RS_1 type (with virtually no late spike-frequency adaptation; Agmon and Connors 1992; Chagnac-Amitai and Connors 1989) and form extensive axonal arbors in layers II/III and usually also in layer V, but largely avoid the layer IV barrels. IG pyramidal neurons, in contrast, form a more heterogeneous group, whose axonal arbors can be oriented either predominantly horizontally within layers V and VI, or predominanly vertically, spanning layers III–VI. They can be of the RS_1 or RS_2 subtypes (the latter showing significant late spike frequency adaptation; Agmon and Connors 1992; Chagnac-Amitai and Connors 1989), and they express biophysical properties uncommon in the superficial layers. In addition to these laminar differences, RS_1 and RS_2 neurons *within* the IG layers are morphologically distinct from each other. Thus subgroups of RS neurons have integrative properties that differ both across and within different laminae and are likely to contribute differently to information processing within the PMBSF. Because laminar location as well as specific constellations of physiological and morphological characteristics distinguish neurons with different extrinsic projections (reviewed in White 1989), these findings also imply that information relayed to different targets is processed differentially within the PMBSF.

Biophysical properties of RS neurons

A central finding of this study is that the relatively subtle differences in firing patterns between RS_1 and RS_2 neurons appear to define two distinct neuronal groups. The former are distributed throughout the extragranular layers, whereas the latter are concentrated in the IG laminae. Similar laminar distributions were reported previously in the rat primary sensory and pyriform cortex (Chagnac-Amitai and Connors 1989; Tseng and Haberly 1989) and in mouse barrel cortex (Agmon and Connors 1992). Furthermore, we show that RS_1 neurons have larger cell bodies and more branched proximal dendritic arbors than RS_2 cells. A neuron's propensity to adapt is likely to be significant for its responses during whisking behavior, with the more strongly adapting RS_2 neurons being well suited to signal the rate of change of an input and the RS_1 neurons providing information about a sustained input. The morphological differences we describe provide further support for the idea that these two groups have specialized contributions to cortical processing.

IG and SG neurons are physiologically distinct. IG neurons – RS_1 and RS_2 alike – show slow inward rectification at hyperpolarized potentials, which is not found in SG neurons. The laminar specificity of this property probably reflects a general feature of cortical organization, as it has been described in several cortical areas of several species (Kasper et al. 1994; Mason and Larkman 1990; Solomon et al. 1993; Williamson and McCormick 1989). In other areas, such rectification was shown to be mediated by a slowly activating Na^+ and K^+ conductance that is partially active at resting potential and fully activated at about –100 mV (I_h. Solomon et al. 1993; Spain et al. 1987). Because of its slow inactivation kinetics, this conductance is likely to shape the neurons' responses to sequential stimuli (Schwindt 1992). In a subset of cortical Betz cells in the cat, for instance, I_h produces a

brief acceleration of firing rate in response to a stimulus that follows a period of hyperpolarization (Spain et al. 1991).

We found that in IG, but not SG, neurons, individual action potentials are followed by DAPs. DAPs were proposed to be mediated by Ca^{2+} conductances and to contribute to intrinsic burst generation (Friedman and Gutnick 1989; Tseng and Haberly 1989). The laminar distribution of cells generating DAPs we found is consistent with that reported in rat pyriform cortex (Tseng and Haberly 1989) but disagrees with a report from rat sensorimotor cortex, where prominent DAPs were recorded from the majority of superficial RS_1 neurons (Chagnac-Amitai and Connors 1989). Further studies are needed to determine whether this discrepancy represents sampling differences among the studies or true areal differences within the neocortex.

Chagnac-Amitai et al. (1990) reported that IG RS neurons project primarily vertically to superficial layers, whereas intrinsically bursting neurons form extensive horizontal axonal arbors. Our findings, however, show that axon collaterals of IG RS neurons – RS_1 and RS_2 alike – project preferentially within their parent layers. Thus RS neurons, which also receive a larger proportion of inhibitory inputs than intrinsically bursting cells (Chagnac-Amitai et al. 1990), may attenuate the reverberatory activity proposed to be initiated in these layers by the strongly interconnected network of intrinsically bursting cells (Chagnac-Amitai and Connors 1989; Chagnac-Amitai et al. 1990; Silva et al. 1991).

Functional aspects of pyramidal neuron morphology

Interpretation of morphological data from tissue slices depends critically on the extent and plane in which neural processes, in particular axons, are truncated by the slice preparation. As the axonal arbors of PMBSF neurons cannot be contained within a slice preparation, any in vitro study must concentrate on a selected portion of these arbors. Based on evidence that intrinsic projections in the PMBSF are oriented preferentially along barrel rows (Bernardo et al. 1990), we chose to describe the axonal arbors of PMBSF neurons along *single barrel rows*. To this end we have devised a plane of section that was parallel to barrel rows. The patterns of axonal arborizations we describe are consistent with results from in vivo extracellular and intracellular dye injections into the PMBSF (Bernardo et al. 1990; Hoeflinger et al. 1995; Ito 1992) and also with results from a large number of cortical areas of several species (Gilbert and Wiesel 1983; Keller and Asanuma 1993; Schwark and Jones 1989; Wallace and Bajwa 1991). Despite the truncation, we often observed axon collaterals that spanned several barrel columns and extended to the end of the PMBSF. These observations suggest that our data provide faithful, if qualitative, descriptions of the intra- and interlaminar projections of PMBSF neurons along single barrel rows. Because of the truncation inherent in the slice preparation, we have chosen to describe *quantitatively* only the neural processes that remained relatively undamaged by slicing – the basal dendrites and proximal 500 μm of the apical dendrites. In drawing qualitative conclusions about the dendritic trees, we screened each neuron and based our conclusions only on those whose dendritic processes terminated within the slice.

The horizontal axon collaterals of the pyramidal cells described here span three to seven barrel columns, a distance at least as large as the receptive fields previously described in these layers (Chapin 1986; Simons 1978). In contrast, the dendritic trees of these neurons are restricted to one or two neighboring columns and are thus smaller than most receptive fields (see also Ito 1992). These findings, together with the fact that surround receptive field responses in PMBSF have longer latencies than responses to center receptive field stimulation, support the hypothesis that the generation of multiwhisker receptive fields is dependent on intracortical, intercolumnar pathways (Armstrong-James et al. 1992). The long horizontal spans of many axon collaterals suggest that they may mediate integration of information not only within but also beyond their receptive fields. Analogous findings were reported for the visual and auditory cortices, where such long-range projections connect neurons with similar functional properties (Gilbert and Wiesel 1989; Matsubara and Phillips 1988). In the barrel cortex such long-range collaterals may connect dispersed neuronal groups that are coactivated during whisking behavior (Nicolelis et al. 1995; see also Gilbert 1992; Keller 1993).

The morphology of layer V neurons suggest that they can receive direct thalamic inputs (from the ventrobasal thalamus, VB either on their basal dendrites and cell bodies in layer V or on their apical dendrites that extend into layer IV (see also Ito 1992; White and Hersch 1982). In contrast, most SG pyramids, whose basal dendrites usually do not reach layer IV, can only receive VB thalamic inputs via the ascending collaterals of neurons in layer V (present study) or of those in layer IV (Valverde 1986). Possible exceptions are neurons located in the lowest portion of layer III, which were not represented in our sample, that receive VB thalamocortical synapses in that layer or on their basal dendrites that may extend into layer IV. These conclusions are supported by electrophysiological data demonstrating a significantly higher incidence of monosynaptic responses to thalamic stimulation among IG cells, compared with SG neurons (Agmon and Connors 1992). In vivo studies also support the existence of a serial interlaminar relay originating in the thalamic termination zones of layers IV and Vb (Chmielowska et al. 1989; Keller et al. 1985). Following stimulation of the principal whiskers in vivo, responses are initiated first in layers IV and Vb followed at longer latencies by responses in layers III, and finally by those in layers II and Va (Armstrong-James et al. 1992; Carvell and Simons 1988; but see Johnson and Alloway 1995). The long-latency responses in layer Va may be mediated by the rich axon collaterals of SG neurons to these layers.

The paucity of axon collaterals in layer IV is consistent with physiological data suggesting that the receptive fields in this layer are relatively independent of long-range intracortical interactions (reviewed in Simons 1995). However, our data show that layer IV does receive some intracortical inputs, primarily from the ascending axon collaterals of IG neurons and, to a lesser extent, through axon collaterals belonging to SG neurons that project horizontally along the superficial and deep borders of layer IV. Though significantly sparser than those in the extragranular layers, these inputs could nevertheless affect neural responses and plasticity in this layer (Armstrong-James 1995; Fox 1994).

Acknowledgements The expert technical assistance of Mr. Daniel Weintraub is sincerely appreciated. Supported by PHS:NINDS grant NS31078. A.K. is an Alfred P. Sloan Research Fellow.

References

Agmon A, Connors BW (1992) Correlation between intrinsic firing patterns and thalamocortical synaptic responses of neurons in mouse barrel cortex. J Neurosci 12:319–329

Armstrong-James M (1995) The nature and plasticity of sensory processing within adult rat barrel cortex. In: Jones EG, Diamond IT (eds) The barrel cortex of rodents. (Cerebral cortex, vol 11) Plenum Press, New York, pp 333–373

Armstrong-James M, Fox K (1987) Spatiotemporal convergence and divergence in the rat SI barrel cortex. J Comp Neurol 263:265–281

Armstong-James M, Fox K, Dasgupta A (1992) Flow of excitation within rat barrel cortex on striking a single vibrissa. J Neurophysiol 68:1345–1358

Bernardo KL, McCasland JS, Woolsey TA, Strominger RN (1990) Local intra- and interlaminar connections in mouse barrel cortex. J Comp Neurol 291:231–255

Brederode JFM van, Snyder GL (1992) A comparison of the electrophysiological properties of morphologically identified cells in layers 5B and 6 of the rat neocortex. Neuroscience 50:315–337

Carvell GE, Simons DJ (1988) Membrane potential changes in rat SmI cortical neurons evoked by controlled stimulation of mystacial vibrissae. Brain Res 448:186–191

Cauller LJ, Connors BW (1994) Synaptic physiology of horizontal afferents to layer I in slices of rat SI cortex. J Neurophysiol 14:751–762

Chagnac-Amitai Y, Connors BW (1989) Synchronized excitation and inhibition driven by intrinsically bursting neurons in neocortex. J Neurophysiol 62:1149–1162

Chagnac-Amitai Y, Luhmann HJ, Prince DA (1990) Burst generating and regular spiking layer 5 pyramidal neurons of rat neocortex have different morphological features. J Comp Neurol 296:598–613

Chapin JK (1986) Laminar differences in sizes, shapes, and response profiles of cutaneous receptive fields in the rat SI cortex. Exp Brain Res 62:549–559

Chapin JK, Sadeq M, Guise JLU (1987) Corticocortical connections with the primary somatosensory cortex of the rat. J Comp Neurol 263:326–346

Chmielowska J, Carvell GE, Simons DJ (1989) Spatial organization of thalamocortical and corticothalamic projection systems in the rat SmI barrel cortex. J Comp Neurol 285:325–338

Connors BW, Gutnick MJ, Prince DA (1982) Electrophysiological properties of neocortical neurons in vitro. J Neurophysiol 48:1302–1320

Fox K (1994) The cortical component of experience-dependent synaptic plasticity in the rat barrel cortex. J Neurosci 14:7665–7679

Friedman A, Gutnick MJ (1989) Intracellular calcium and control of burst generation in neurons of guinea-pig neocortex in vitro. Eur J Neurosci 1:374–381

Gilbert CD (1992) Horizontal integration and cortical dynamics. Neuron 9:1–13

Gilbert CD, Wiesel TN (1983) Clustered intrinsic connections in cat visual cortex. J Neurosci 3:1116–1133

Gilbert CD, Wiesel TN (1989) Columnar specificity of intrinsic horizontal and corticocortical connections in cat visual cortex. J Neurosci 9:2343–2442

Gutnick MJ, Crill WE (1995) The cortical neuron as an electrophysiological unit. In: Gutnick MJ, Modi I (eds) The cortical neuron. Oxford University Press, New York, pp 33–51

Hoeflinger BF, Bennett-Clarke CA, Chiaia NL, Killackey HP, Rhoades RW (1995) Patterning of local intracortical projections within the vibrissae representation of rat primary somatosensory cortex. J Comp Neurol 354:551–563

Ito M (1992) Simultaneous visualization of cortical barrels and horseradish peroxidase-injected layer-5b vibrissa neurones in the rat. J Physiol (Lond) 454:247–265

Johnson MJ, Alloway KD (1995) Evidence for synchronous activation of neurons located in different layers of primary somatosensory cortex. Somatosens Mot Res 12:235–247

Jones EG, Diamond IT (1995) The barrel cortex of rodents. (Cerebral cortex, vol 11) Plenum Press, New York

Kaspar EM, Larkman AU, Lübke J, Blakemore C (1994) Pyramidal neurons in layer 5 of the rat visual cortex. I. Correlation among cell morphology, intrinsic electrophysiological properties, and axon targets. J Comp Neurol 339:459–474

Keller A (1993) Intrinsic synaptic organization of the motor cortex. Cereb Cortex 3:430–441

Keller A (1995) Synaptic organization of the barrel cortex. In: Jones EG, Diamond IT (eds) The barrel cortex of rodents. (Cerebral cortex, vol 11) Plenum Press, New York, pp 221–262

Keller A, Asanuma H (1993) Synaptic relationships involving local axon collaterals of pyramidal neurons in the cat motor cortex. J Comp Neurol 336:229–242

Keller A, White EL, Cipolloni PB (1985) The identification of thalamocortical axon terminals in barrels of mouse SmI cortex using immunohistochemistry of anterogradely transported lectin (*Phaseolus vulgaris* lecoagglutinin). Brain Res 343:159–165

Killackey HP, Leshin S (1975) The organization of specific thalamocortical projections to the posteromedial barrel subfield of the rat somatic sensory cortex. Brain Res 86:469–472

Kyriazi HT, Carvell GE, Brumberg JC, Simons DJ (1996) Quantitative effects of GABA and bicuculline methiodide on receptive field properties of neurons in real and simulated barrels. J Neurophysiol 75:547–560

Mason A, Larkman A (1990) Correlations between morphology and electrophysiology of pyramidal neurons in slices of rat visual cortex. II. Electrophysiology. J Neurosci 10:1415–1428

Matsubara JA, Phillips DP (1988) Intracortical connections and their physiological correlates in the primary auditory cortex (AI) of the cat. J Comp Neurol 268:38–48

McCormick DA, Connors BW, Lighthall JW, Prince DA (1985) Comparative electrophysiology of pyramidal and sparsely spiny stellate neurons of the neocortex. J Neurophysiol 54: 782–805

Nicolelis MAL, Baccala LA, Lin RCS, Chapin JK (1995) Sensorimotor encoding by synchronous neural ensemble activity at multiple levels of the somatosensory system. Science 268: 1353–1358

Schwark HD, Jones EG (1989) The distribution of intrinsic cortical axons in area 3b of cat primary somatosensory cortex. Exp Brain Res 78:501–513

Schwindt PC (1992) Ionic currents governing input-output relations of Betz cells. In: McKenna T, Davis J, Zornetzer SF (eds) Single neuron computations. Academic Press, San Diego

Senft SL, Woolsey TA (1991) Growth of thalamic afferents into the mouse barrel cortex. Cereb Cortex 1:308–335

Sholl DA (1953) Dendritic organization in the neurons of the visual and motor cortices of the cat. J Anat 87:387–407

Silva LR, Amitai Y, Connors BW (1991) Intrinsic oscillations of neocortex generated by layer 5 pyramidal neurons. Science 251:432–435

Simons DJ (1978) Response properties of vibrissa units in rat SI somatosensory neocortex. J Neurophysiol 41:798–820

Simons DJ (1995) Neuronal integration in the somatosensory whisker/barrel cortex. In: Jones EG, Diamond IT (eds) The barrel cortex of rodents. (Cerebral cortex, vol 11) Plenum Press, New York, pp 263–297

Simons DJ, Carvell GE, Hershey AE, Bryant DP (1992) Responses of barrel cortex neurons in awake rats and effects of urethane Anesthesia. Exp Brain Res 91:259–272

Solomon JS, Doyle JF, Burkhalter A, Nerbonne JM (1993) Differential expression of hyperpolarization-acitvated currents reveals distinct classes of visual cortical projection neurons. J Neurosci 13:5082–5091

Spain WJ, Schwindt PC, Crill WE (1987) Anomalous rectification in neurons from cat sensorimotor cortex in vivo. J Neurophysiol 57:1555–1576

Spain WJ, Schwindt PC, Crill WE (1991) Post-inhibitory excitation and inhibition in layer V pyramidal neurones from cat sensorimotor cortex. J Physiol (Lond) 434:609–626

Tseng GF, Haberly LB (1989) Deep neurons in piriform cortex. II. Membrane properties that underlie unusual synaptic responses. J Neurophysiol 62:386–400

Valverde F (1986) Intrinsic neocortical organization: some comparative aspects. Neuroscience 18:1–23

Wallace MN, Bajwa S (1991) Patchy intrinsic connections of the ferret primary auditory cortex. Neuroreport 2:417–420

Welker C, Woolsey TY (1974) Structure of layer IV in the somatosensory neocortex of the rat: description and comparison with the mouse. J Comp Neurol 158:437–454

White EL (1989) Cortical circuits: synaptic organization of the cerebral cortex – structure, function and theory. Birkhäuser, Boston

White EL, Hersch SM (1982) A quantitative study of thalamocortical and other synapses involving the apical dendrites of corticothalamic projection cells in mouse SmI cortex. J Neurocytol 11:137–157

Williamson A, McCormick DA (1989) Inward rectification varies with cortical lamina in guinea-pig neocortical neurons in vitro. Soc Neurosci Abstr 15:1309

Wong-Riley M (1979) Changes in the visual system of monocularly suture or enucleated cats demonstrated with cytochrome oxidase histochemistry. Brain Res 171:11–28

Woolsey TA, Van der Loos H (1970) The structural organization of layer IV in the somatosensory region (SI) of mouse cerebral cortex. Brain Res 17:205–242